Interference of Neuronal TrkB Signaling by the Cannabis-Derived Flavonoids Cannflavins A and B

Jennifer Holborn[1*], Alicyia Walczyk-Mooradally[1*], Colby Perrin[1], Begüm Alural[1], Cara Aitchinson[1], Jibran Y. Khokar[2], Tariq A. Akhtar[1], Jasmin Lalonde[1]

[1] Department of Molecular and Cellular Biology, University of Guelph, 50 Stone Road E, Guelph, ON N1G 2W1, Canada.

[2] Department of Biomedical Science, University of Guelph, 50 Stone Road E, Guelph, ON N1G 2W1, Canada

* J.H. and A.W.M. contributed equally to this report.

Correspondence to: **Jasmin Lalonde**

Email: jlalon07@uoguelph.ca
Phone: (519) 824-4120 x. 54706
ORCID: 0000-0002-6797-1894

Keywords: Cannflavins; Flavanoids; TrkB; BDNF; Arc

ABSTRACT

Cannflavins A and B are two flavonoids that accumulate in the *Cannabis sativa* plant. These specialized metabolites are uniquely prenylated and highly lipophilic, which, *a priori*, may permit their interaction with membrane-bound enzymes and receptors. Although previous studies found that cannflavins can produce anti-inflammatory responses by inhibiting the biosynthesis of pro-inflammatory mediators, the full extent of their cellular influence remains to be understood. Here, we studied these flavonoids in relation to the Tropomyosin receptor kinase B (TrkB), a receptor tyrosine kinase that is activated by the growth factor brain-derived neurotrophic factor (BDNF). Using mouse primary cortical neurons, we first collected evidence that cannflavins prevent the accumulation of Activity-regulated cytoskeleton-associated (Arc) protein upon TrkB stimulation by exogenous BDNF in these cells. Consistent with this effect, we also observed a reduced activation of TrkB and downstream signaling effectors that mediate *Arc* mRNA transcription when BDNF was co-applied with the cannflavins. Of note, we also performed a high-throughput screen that demonstrated a lack of agonist action of cannflavins towards 320 different G protein-coupled receptors, a result that specifically limit the possibility of a TrkB transinactivation scenario via G protein signaling to explain our results with dissociated neurons. Finally, we used Neuro2a cells overexpressing TrkB to show that cannflavins can block the growth of neurites and increased survival rate produced by the higher abundance of the receptor in this model. Taken together, our study offers a new path to understand the reported effects of cannflavins and other closely related compounds in different cellular contexts.

INTRODUCTION

Flavonoids are polyphenolic compounds found in various plant-derived foods and beverages. These phytochemicals represent a large family of molecules that can be classified into six main subclasses, based on their chemical structure: flavonols, flavanols (also known as flavan-3-ols or catechins), flavanones, flavones, anthocyanins, and isoflavones (Panche et al., 2016). Interestingly, evidence suggests that moderate habitual intake of flavonoids can lower the risk of cardiovascular disease, cancer, as well as all-cause mortality (Bondonno et al., 2019). Another purported benefit of these natural products is their positive influence on brain health and function, as several members of the flavonoid family have been found to promote neuroprotection, reduce neuroinflammation, and enhance cognition (Vauzour et al., 2008; Jaeger et al., 2018; Bakoyiannis et al., 2018). More precisely, flavonoids appear to modulate signaling pathways that are central to the control of neuronal survival and plasticity, such as the MAPK-CREB and PI3K-mTOR cascades (Vauzour et al., 2008; Jaeger et al., 2018). However, this particular line of inquiry has been little studied and therefore represents an opportunity to identify new bioactive compounds with therapeutic qualities among this family of phytochemicals.

Apart from the psychoactive molecule Δ^9-tetrahydrocannabinol (THC) and other related cannabinoids with only mild or no psychotropic effect, like cannabidiol (CBD) and cannabigerol (CBG), the *Cannabis sativa (C. sativa)* plant also produces hundreds of specialized metabolites including at least twenty different flavonoid compounds (Flores-Sanchez et al., 2008). Among those, the flavones cannflavin A and cannflavin B (Figure 1A) are considered to accumulate uniquely in *C. sativa* cultivars. Seminal work by Barrett and colleagues performed more than 30 years ago helped identify these two flavonoids and characterize them as inhibitors of prostaglandin E_2 production with the ability to produce anti-inflammatory effects that are approximately thirty

58 times more potent than acetylsalicylic acid, better known as aspirin (Barrett et al., 1985; 1986).
59 However, a broader understanding of cannflavins' influence on cell biology in health and disease
60 did not progress much since their initial description because of challenges associated with their
61 extraction and the various political landscapes that limited their distribution. Nevertheless, some
62 pre-clinical studies have provided intriguing new details about these molecules in recent years. For
63 instance, the unnatural isomer of cannflavin B named FBL-03G (also known as caflanone) was
64 found to increase apoptosis of pancreatic cancer cells *in vitro* while animal tests showed that the
65 same small molecule could limit progression of metastatic pancreatic cancer (Moreau et al., 2019).
66 Additionally, another study reported a possible neuroprotective effect of cannflavin A at
67 concentrations lower than 10 μM that was attributed to the ability of this molecule to reduce
68 aggregation of β amyloid through direct docking in the hydrophobic groove of the protein (Eggers
69 et al., 2019). While these different findings provide novel insights about the pharmacological
70 potential of cannflavins, the full range of molecular changes induced by cannflavins in cells
71 remains to be described. To address this gap in our understanding of cannflavin pharmacology, we
72 therefore focused on identifying novel mechanisms of action of these two related cannabis-derived
73 metabolites in neuronal cells.

74 Cannflavins A and B are prenylated and highly lipophilic small molecules (Barrett et al., 1985;
75 Choi et al., 2004), a characteristic that allows them to easily accumulate into cells where they can
76 then presumably interact with different membrane-bound enzymes and receptors. Previously, we
77 published a chemogenomic analysis that aimed at identifying small molecule modulators of
78 Activity-regulated cytoskeleton-associated protein (Arc), which is a key regulator of
79 neuroplasticity and cognitive functions (Bramham et al., 2010; Korb et al., 2011; Kedrov et al.,
80 2019). Our approach in that project exploited the ability of the growth factor brain-derived

neurotrophic factor (BDNF) to promote abundant *Arc* mRNA expression followed by nuclear accumulation of the protein product in mouse primary cortical neurons via activation of Tropomyosin receptor kinase B (TrkB) receptor (Lalonde et al., 2017). Here, we have adapted this assay to test the two cannflavins and found evidence of TrkB signaling interference by both molecules. These results then led us to complete a secondary high-throughput screen to test possible agonist activity of these flavonoids on G protein-coupled receptors (GPCRs), as well as other biochemical assays to confirm the influence of cannflavins and pinpoint their potential target engagement. These specific efforts suggest a model where cannflavins interfere with TrkB activity through direct inhibitory action on the receptor. Finally, image-based cellular test with immortalized Neuro2a cells ectopically expressing TrkB allowed us to demonstrate the capacity of cannflavins to block BDNF-induced neurite outgrowth. In summary, our study supports the classification of cannflavins as candidate inhibitors of TrkB receptor signaling in neuronal cells.

METHODS

Cell culture and transfection

Developing cerebral cortex from E16.5 CD-1 mouse embryos were dissected and then dissociated in trypsin solution for 15 min followed by three washes with phosphate-buffered saline (PBS). Trypsinized tissue was gently triturated to produce single cell suspension. Next, cells were seeded in poly-L-lysine/laminin coated 6-well plates at a density of 1.5×10^6 per well and maintained in Neurobasal medium containing B27 supplement (2%, Invitrogen, Grand Island, NY), penicillin (50 U/ml, Invitrogen), streptomycin (50 µg/ml, Invitrogen) and glutamine (1 mM, Sigma). For experiments involving BDNF (PeproTech, Rocky Hill, NJ), the growth factor was added directly to the culture medium at a final concentration of 100 ng/ml for the indicated period of time.

Preparation of mouse primary cortical neuron cultures was approved by the University of Guelph Animal Care Committee and carried out according to institutional guidelines.

For neurite outgrowth assay, Neuro2a cells were cultured in DMEM [supplemented with 10% HyClone FetalClone II serum (Cytiva, Global Life Sciences Solutions, Marlborough, MA), penicillin (50 units/ml), and streptomycin (50 µg/ml)] and transfected overnight using Lipofectamine 2000 (Invitrogen) according to the manufacturer's protocol.

Antibodies, plasmid, and pharmacological compounds

The anti-Arc rabbit polyclonal affinity purified antibody (#156 003) was purchased from Synaptic Systems (Goettingen, Germany). The antibodies recognizing p42 Mapk (Erk2, sc-1647) was from Santa Cruz Biotechnology (Santa Cruz, CA). The antibodies recognizing phosphorylated TrkA^{Tyr490}/TrkB^{Tyr516} (#4619), phosphorylated p44/42 Mapk (Erk1/2$^{Thr202/Tyr204}$, #4370), Akt (#4691), phosphorylated Akt^{Thr308} (#2965), phosphorylated Akt^{Ser473} (#4060), mTor (#2983), phosphorylated mTor^{Ser2448} (#2971), and phosphorylated rpS6$^{Ser240/244}$ (#2215) were acquired from Cell Signaling Technology (Beverly, MA). The antibodies recognizing TrkB (MAB397) were acquired from R&D Systems (Minneapolis, MN). The antibodies recognizing β-actin (A1978) and M2 FLAG (F1804) antibodies were from Sigma-Aldrich (St-Louis, MO), while the Map2 (AB5543) antibody was purchased from EMD Millipore Corps (Billerica, MA). Finally, cross-absorbed horseradish peroxidase-conjugated secondary antibodies were from Invitrogen.

The pCMV6-Ntrk2-Myc-DDK (FLAG) plasmid (MR226130) was purchased from OriGene Biotechnologies (Rockville, MD). ECGC, genistein, and daidzein were from Sigma-Aldrich. ANA-12 (Figure 1B) was from Tocris Bioscience (Bristol, UK) and U0126 was from Biosciences (Thermo Fisher).

The synthesis and purification of cannflavins A and B were produced using the method of Rea and colleagues (2019). Briefly, *Cannabis sativa* L. prenyltransferase 3 (CsPT3) was recombinantly expressed in *Saccharomyces cerevisiae* and the microsomal fraction containing CsPT3 was collected for *in vitro* enzyme assays. Assays containing 200 µM chrysoeriol, 400 µM GPP or DMAPP, 1 mg/mL of microsomal protein, and 10 mM $MgCl_2$ in 100 mM Tris-HCl buffer were conducted at 37ºC for 120 min and terminated with the addition of 20% formic acid. Cannflavin products were extracted with three volumes of ethyl acetate, the organic layer was dried under N_2 gas and resuspended in methanol. The products were purified by HPLC on an Agilent 1260 Infinity system equipped with a Waters SPHERISORB 5 µm ODS2 column, and eluted with a 20 min linear gradient from 45% to 95% methanol in water containing 0.1% formic acid. Product identities were confirmed via LC-MS according to published methods (Rea et al., 2019) (Supplementary Figure 1). Cannflavins produced *in vitro* were dried under nitrogen gas and resuspended in dimethyl sulfoxide (DMSO). The final products were confirmed via HPLC, as described above, and quantified by absorption at 340 nm relative to authentic standards.

Western blotting

For western blot analyses, cells were collected by scraping in ice-cold radioimmunoprecipitation assay (RIPA) buffer (50 mM tris-HCl [pH 8.0], 300 mM NaCl, 0.5% Igepal-630, 0.5% deoxycholic acid, 0.1% SDS, 1 mM EDTA) supplemented with a cocktail of protease inhibitors (Complete Protease Inhibitor without EDTA, Roche Applied Science, Indianapolis, IN) and phosphatase inhibitors (Phosphatase Inhibitor Cocktail 3, Sigma-Aldrich). One volume of 2× Laemmli buffer (100 mM tris-HCl [pH 6.8], 4% SDS, 0.15% bromophenol blue, 20% glycerol, 200 mM β-mercaptoethanol) was added and the extracts were boiled for 5 min. Samples were

adjusted to an equal concentration after protein concentrations were determined using the BCA assay (Pierce, Thermo Fisher Scientific). Lysates were separated using SDS–PAGE (polyacrylamide gel electrophoresis) and transferred to a nitrocellulose membrane. After transfer, the membrane was blocked in TBST (tris-buffered saline and 0.1% Tween 20) supplemented with 5% nonfat powdered milk and probed with the indicated primary antibody at 4°C overnight. After washing with TBST, the membrane was incubated with the appropriate secondary antibody and visualized using enhanced chemiluminescence (ECL) reagents according to the manufacturer's guidelines (Pierce, Thermo Fisher Scientific).

The following procedure was used to quantify western blot analyses. First, equal quantity of protein lysate as determined by the BCA assay was analyzed by SDS-PAGE for each biological replicate. Second, the exposure time of the film to the ECL chemiluminescence was the same for each biological replicate. Third, all the exposed films were scanned on a HP Laser Jet Pro M377dw scanner in grayscale at a resolution of 300 dpi. Fourth, the look-up table (LUT) of the scanned tiff images was inverted and the intensity of each band was individually estimated using the selection tool and the histogram function in Adobe Photoshop CC 2021 software. Finally, the intensity of each band was divided by the intensity of its respective loading control (β-actin) to provide the normalized value used for statistical analysis.

Immunocytochemistry

Indirect immunofluorescence detection of antigens was carried out using cortical neurons cultured on poly-L-lysine/laminin coated coverslips in 24-well plates at a density of 0.1×10^6 per well. After experimental treatment, cells were washed twice with phosphate-buffered saline (PBS) and fixed for 30 min at room temperature with 4% paraformaldehyde in PBS. After fixation, cells were

washed twice with PBS, permeabilized with PBST (PBS and 0.25% Triton X-100) for 20 min, blocked in blocking solution (5% goat non-immune serum in PBS) for another 30 min, and finally incubated overnight at 4°C with the first primary antibody in blocking solution. The next day, coverslips were extensively washed with PBS and incubated for 2 hours at room temperature in the appropriate fluorophore-conjugated secondary antibody solution [Alexa Fluor 488-, Alexa Fluor 594, or Alexa Fluor 647-conjugated secondary antibody (Molecular Probes, Invitrogen) in blocking solution]. After washes with PBS, the coverslips were incubated again overnight in primary antibody solution for the second antigen, and the procedure for conjugation of the fluorophore-conjugated secondary antibody was repeated as above. Finally, cell nuclei were counterstained with 4′,6-diamidino-2-phenylindole (DAPI), and coverslips were mounted on glass slides with ProLong Antifade reagent (Invitrogen).

Cells cultured on coverslips from three independent biological replicates were imaged with a Nikon Eclipse Ti2-E inverted microscope equipped with a motorized stage, image stitching capability, and a 60× objective (Nikon Instruments, Melville, NY). Image analysis was performed with ImageJ and NIS Elements and the following procedure was used to quantify nuclear Arc level in response to BDNF-TrkB signaling. First, original raw tiff files were opened and the nucleus of all neurons in the image was located based on Map2 immunostaining, then average pixel intensity corresponding to Arc immunofluorescence was measured for a 30-pixel spot positioned at the center of the nuclear compartment. Second, for each measure of Arc nuclear immunofluorescence pixel intensity, a measure of background pixel intensity from the same image channel was acquired and subsequently subtracted from the Arc nuclear immunofluorescence pixel intensity value. Finally, Arc immunofluorescence signal from untreated samples was used to establish an objective threshold (two standard deviations above the nuclear Arc immunofluorescence signal averaged

196 from a representative population of untreated neurons) which allowed for comparison of nuclear
197 Arc expression between different experimental conditions.
198
199 *Real-time reverse transcriptase PCR*
200 After experimental treatment, total RNA was isolated from primary cortical neuron cultures using
201 the TRIzol method (Invitrogen). The concentration of total RNA was measured using a NanoDrop
202 ND-8000 spectrophotometer (Thermo Fisher Scientific) and first-strand complementary DNA
203 (cDNA) was synthesized using the iScript cDNA Synthesis Kit (Bio-Rad, Hercules, CA). Real-
204 time PCRs were performed using gene-specific primers and monitored by quantification of SYBR
205 Green I fluorescence using a Bio-Rad CFX96 Real-Time Detection System. Expression was
206 normalized against *Gapdh* expression. The relative quantification from three biological replicates
207 was calculated using the comparative cycle threshold ($\Delta\Delta C_T$) method.
208 Primers for real-time reverse transcription PCR experiments were: *Arc* primer pair one, 5′-
209 TAGCCAGTGACAGGACCCAG-3′ (forward) and 5′-CAGCTCAAGTCCTAGTTGGCAAA-3′ (reverse);
210 *Arc* primer pair two, 5′- CGCCAAACCCAATGTGATCCT-3′ (forward) and 5′-
211 TTGGACACTTCGGTCAACAGA-3′ (reverse); *Gapdh*, 5′-ATGACCACAGTCCATGCCATC-3′ (forward)
212 and 5′-CCAGTGGATGCAGGGATGATGTTC-3′ (reverse).
213
214 *PRESTO-Tango GPCR assay*
215 Parallel receptorome expression and screening via transcriptional output, with transcription
216 activation following arresting translocation (PRESTO-Tango) was used to assess cannflavin A and
217 cannflavin B potential to stimulate G protein-coupled receptors (GPCRs) according to published
218 methods (Kroeze et al., 2015). Overall, 320 distinct nonolfactory human GPCRs were tested.
219

Neurite outgrowth assessment

Neuro2A cells transfected with a pCMV6-Ntrk2-Myc-DDK (FLAG) construct were selected with G-418 (Geneticin) to produce a stable cell line that constitutively expresses Myc-FLAG tagged-TrkB. For neurite outgrowth assessment, cells were seeded on 15 mm glass coverslips in 12-well plates at a density of 2.0×10^4 per well and allowed to attach overnight. Next day, cells were treated with recombinant BDNF (1 nM) plus cannflavins (10 µM), ANA-12 (10 µM), or vehicle control (DMSO). Phase contrast digital images were collected with a Nikon Eclipse Ti2-E inverted microscope and a 20× objective 24 hours after start of treatment (five fields per dish, three wells per condition). Image analysis was completed using ImageJ software using the following procedure. First, any cells with a fragmented nucleus were excluded from the analysis, therefore the total number of viable cells was counted per field. Second, for all identified viable cells the total number of neurites and number of cells with neurites longer than 2 cell bodies in diameter were counted per field.

Statistics

Unless mentioned otherwise, all results represent the mean ±SEM from at least three independent experiments. ANOVA followed by Tukey's or Dunnett's post hoc test for multiple comparisons were performed where indicated.

RESULTS

Impact of cannflavins on BDNF-induced Arc expression in mouse primary cortical neurons

Previously, we completed a chemogenomic screen with primary mouse cortical neurons that identified a suite of compounds that acted as Arc expression modifiers (Lalonde et al., 2017). Part

of this group included five distinct flavonoids (Figure 1C)—namely (–)-epigallocatechin (ECGC), baicalin (BAI), 7,8-dihydroxyflavone (7,8-DHF), daidzein, and genistein—which were found to enhance nuclear Arc protein levels above the control measure when co-applied at a final concentration of 16.7 µM with recombinant BDNF for 6 h. Searching for a possible explanation to this phenomenon, we were intrigued by several studies that had linked each of these five flavonoids to either enhancement of *BDNF* and/or *TrkB* mRNA expression, or to the potentiation of downstream TrkB-dependent signaling (Pan et al., 2012; Gundimeda et al., 2014; Ding et al., 2018; Lu et al., 2019). Based on these observations, we hypothesized that cannflavin A and cannflavin B could act in a similar fashion and promote Arc protein abundance when added to cultured mouse cortical neurons that were stimulated with exogenous BDNF. Unexpectedly, though, western blot analysis assessing BDNF-induced Arc expression in conjunction with cannflavins with concentrations of the flavonoids ranging between 1 to 20 µM revealed an opposite effect. Specifically, we found that application of cannflavins to cell culture media prevented the normal increase in Arc protein by BDNF in a dose-dependent manner where 10-20 µM of cannflavin A, and all tested concentrations (1-20 µM) of cannflavin B, resulted in significantly less Arc protein abundance than seen in the BDNF-alone control measure (Figure 2A). To further support this result, we repeated the experiment using fluorescent immunocytochemistry and quantified nuclear Arc changes, as we had done previously in our chemogenomic screen (Lalonde et al., 2017). Of note, we also tested the flavonol ECGC, as well as the isoflavone daidzein and genistein, since those molecules were found to produce the opposite effect of increasing BDNF-induced nuclear Arc levels according to our previous screening results. As shown in Figure 2B and Supplementary Figure 2, cells that were co-treated with BDNF and 10 µM daidzein or genistein presented a moderate increase in the percentage of nuclei with Arc expression above

threshold in comparison to the BDNF-alone control. Interestingly, though, the ECGC condition was similar on average to the BDNF-alone condition suggesting that the final concentration of this specific flavonoid must be greater than 10 μM to have an impact of TrkB-induced nuclear Arc level. Most importantly, and consistent with our western blot analysis above, cultures treated with BDNF and 1-10 μM cannflavins presented similar overall trends in the reduction of Arc-positive neuronal abundance in comparison to the unstimulated control (Figure 2C). Together, these results confirm the observed discrepancy between cannflavins and the other flavonoids found in our earlier screen, which focused on BDNF-induced Arc expression modifiers.

Next, to ascertain whether the cannflavins' influence on TrkB signaling and Arc protein levels was produced before or after gene transcription, we performed a quantitative polymerase chain reaction (qPCR) experiment using two pairs of primers targeting different regions of the *Arc* transcript. Here, comparison of *Arc* mRNA abundance between untreated, BDNF-alone control, and BDNF with cannflavin A (10 μM) or cannflavin B (10 μM) samples clearly indicated that cannflavins prevent induction of *Arc* mRNA expression (Figure 2D), therefore suggesting that the effect of these compounds must occur somewhere between the activation of TrkB receptors by BDNF and the activation of the transcriptional machinery involved in *Arc* expression.

Evaluating agonist potential of cannflavins on Tango GPCR assay

Considering the transactivation crosstalk between GPCRs and receptor tyrosine kinases, including TrkB (Rajagopal et al., 2004; 2006; El Zein et al., 2007), and recent evidence for GPCR modulation/self-association by flavonoids on the latter (Herrera-Hernández et al., 2017; Ortega et al., 2019), we speculated that one mechanism by which cannflavins could interfere on *Arc* mRNA expression in cortical neurons involves activation of a G protein signal that transinactivates the

function of molecular cascades downstream of TrkB receptors responsible for *Arc* expression. To explore this scenario, we tested the effect of cannflavins on the GPCRome, *en masse,* using the PRESTO-Tango assay—an unbiased high-throughput screening approach adapted to identify agonist activity of agents towards the large family of GPCRs (Kroeze et al, 2015). Interestingly, applying cannflavin A revealed no effect on any of the 320 different GPCRs tested while cannflavin B was found to produce only weak increase (4.4 fold-change) of GPR150 activity from baseline, a negligible effect in comparison to the positive control (51.3 fold-change, dopamine D_2 receptor stimulated by quinpirole) (Figure 3). Faced with these results, we then re-focused our attention on the possibility that cannflavins act more directly on the TrkB receptor and/or its downstream signaling components.

Elucidating cannflavins effects on TrkB signaling

BDNF binding to the extracellular domain of a TrkB receptor stimulates its dimerization and the phosphorylation of intracellular tyrosine residues which is followed by the recruitment of pleckstrin homology (PH) and SH2 domain containing proteins—such as FRS2, Shc, SH2B, and SH2B2—that regulate distinct concurrent signaling cascades (Qian et al., 1998; Meakin et al., 1999). To explore whether cannflavins interfere with the activation of TrkB receptors by BDNF in primary cortical neurons, we used a western blotting approach and probed lysates with a P-TrkA/B antibody. This approach revealed that, indeed, cannflavins can prevent BDNF from effectively stimulating its target receptor (Figure 4A). To further support this result, we tested the activation of signaling pathways that are likely regulated downstream of TrkB, including the Ras-Raf-MEK-Mapk and the PI3K/Akt/mTor cascades (Huang et al., 2003; Kowiański et al., 2018) (Figure 4B). Interestingly, our analyses revealed that both cannflavin A and cannflavin B sharply

reduced normal increase in P-Mapk, P-Akt, P-mTor, and P-rpS6 levels produced by BDNF (Figure 4C). The fact that there were those changes in these three molecular pathways, which to a great extent occurs in parallel with limited cross-interaction (Kowiański et al., 2018), strongly suggest that cannflavins must act at an early stage in TrkB signal activation.

Functional characterization TrkB inhibition by cannflavins on BDNF-dependent neurite outgrowth

Our biochemical analyses with mouse primary cortical neurons suggest that cannflavins A and B have inhibitory activity towards TrkB receptors. In order to establish if this effect is sufficient to limit cellular processes under the control of BDNF signaling, we used neuroblastoma Neuro2a cells stably expressing Ntrk2 (TrkB)-Myc-FLAG to complete a neurite outgrowth experiment (Figure 5A). As shown in Figure 5B, Neuro2a cells have low TrkB expression with negligeable phosphorylation of the receptor under basal conditions, while cells stably expressing the receptor display greater responsiveness to exogenous application of BDNF—which is clearly demonstrated by higher level of P-TrkB. Further, pre-application of cannflavins (20 μM) with BDNF to the culture media for 6 h reduced BDNF-induced TrkB phosphorylation (Figure 5C). Interestingly, we did not observe a decrease in P-Mapk levels with treatment of ANA-12 or cannflavins as was observed in cortical neurons (Figure 4C), a distinction that we attribute to the fact that overexpression of TrkB in Neuro2A produced maximal phosphorylation of the p-42 subunit of Mapk and no change in signal when BDNF was added to the Neuro2a cells (Figure 5B). Most importantly, neurite assays completed with and without the application of ANA-12, cannflavin A, and cannflavin B revealed that all three compounds produced a significant decrease in the total number of neurites per field (Figure 5D and E) and number of cells with processes twice the length

of the cell (Figure 5F) when applied at a final concentration of 10 µM to culture media. We also noticed a significant decrease in viable cells (Figure 5G) at this same concentration but only between the BDNF control condition and the BDNF plus ANA-12 or cannflavins. Of note, our measures of total number and length of neurites, as well as cell survival, for the ANA-12 and cannflavins conditions in this experiment were comparable to the baseline values were observed in wild-type Neuro2a cells not overexpressing TrkB (Supplementary Figure 3). Altogether, our results here strongly support that cannflavins act on TrkB receptors, preventing BDNF activation of downstream signaling of the receptor.

DISCUSSION

This study provides evidence for an inhibitory effect of cannflavins A and B, two flavonoids from *C. sativa*, on BDNF-induced Arc expression through disruption of TrkB receptor signaling. These results contrast our previous observations that various flavonoids exhibit a potentiating effect towards BDNF-induced Arc accumulation in mouse primary cortical neurons (Lalonde et al., 2017). Strikingly, the addition of cannflavin A or cannflavin B to the culture medium of mouse primary cortical neurons at a minimum concentration of 5 µM consistently prevented the induction of *Arc* mRNA expression, suggesting that these molecules act between BDNF-activation of TrkB receptors and transcription of the *Arc* gene. Therefore, we subsequently investigated the impact of cannflavins on the downstream pathways of TrkB using biochemical analyses and uncovered a consistent decrease in the activation of the Ras-Raf-Mek-Mapk and the PI3K/Akt/mTor cascades. In connection with these results, we demonstrated that cannflavins inhibited BDNF-induced neurite outgrowth in neuroblastoma Neuro2a cells stably overexpressing TrkB. Taken together, our study provides a new path to better understand the effects that have been reported in recent

years about cannflavins and other closely related compounds against certain cancer cell types (Brunelli et al., 2009; Moreau et al., 2019).

Structural determinants of cannflavins activity towards TrkB

All flavonoids have a basic flavan nucleus with two aromatic rings (the A and the B rings) interconnected by a three-carbon-atom heterocyclic ring (the C ring), as illustrated in Figure 1C for the flavone 7,8-dihydroxyflavone (7,8-DHF, also known as tropoflavin). Interestingly, a previous study focusing on 7,8-DHF, which is a compound reported to mimic the physiological activity of BDNF and stimulate TrkB signaling *in vitro* and *in vivo* (Jang et al., 2010; Zeng et al., 2012), helps speculate about what precise structural feature might confers TrkB antagonistic activity to cannflavins. Specifically, previous comparison of different 7,8-DHF derivatives on TrkB phosphorylation and downstream Akt signaling revealed that the presence of a 3'-hydroxy group (or to a lesser extent a 2'-hydroxy group) on the B ring confers a TrkB stimulatory effect to a 7,8-DHF derivative compound whereas addition of a 4'-hydroxy group, as shown in Figure 6A with 7, 8, 4'-trihydroxyflavone and Figure 6B with 3, 5, 7, 8, 3, 4'-hexahydroxyflavone, inversely mediates inhibition of the receptor (Liu et al., 2010). Since cannflavins A and B are both hydroxylated at the 4' position on the B ring (Figure 1A), similar to compounds found by Liu and colleagues (2010) interfering with TrkB phosphorylation in rat primary cortical neurons (Figures 6A and 6B), we thus suspect that this specific structural feature is key in mediating the TrkB antagonistic effect observed in our study. In this context, it will be revealing whether cannflavin derivatives with different patterns of hydroxylation on the B ring produce a different activity towards TrkB and downstream cellular effects.

In addition to 4' hydroxylation of the B ring, prenylation is another structural element that we must consider in relation to the difference we consistently observed between cannflavin A and cannflavin B towards TrkB. As seen in Figure 1A, cannflavin B has only one isoprene unit while cannflavin A has two, making the later an overall larger and more lipophilic molecule. Consequently, we speculate that the smaller size of cannflavin B may facilitate access and/or create a stronger binding affinity to TrkB in a cellular context, which could then explain why we have been measuring a more potent inhibitory response of the receptor phosphorylation and blunting of downstream signaling with this specific compound. Here, though, we also need to acknowledge the fact that our data do not demonstrate direct interaction of cannflavins A and B with TrkB at this point. Nevertheless, two specific results from our study support to a certain degree the idea that a direct functional interaction most likely occur between cannflavins and TrkB. First, our interrogation of the GPCRome using the PRESTO-Tango assay showed that cannflavins do not stimulate the activity of more than 300 GPCRs, which rules out the possibility that cannflavins are disrupting TrkB function through a GPCR transinactivation event in our cellular experiments (Rajagopal et al., 2004; 2006; El Zein et al., 2007). And second, our experiment with Neuro2a cells stably expressing TrkB reveals that cannflavins block the growth of neurites, as well as the observed cell survival stimulatory effect, produced by exogenous BDNF application in this model. Since these phenotypes are directly tied to the overexpression of TrkB, and that application of cannflavins consistently returns neurite and survival measures to those of wild-type Neuro2a cells (Supplementary Figure 3), we consider these results as evidence for a direct interaction between cannflavins and TrkB. To conclude on this point, whether the activity of receptor tyrosine kinases other than TrkB is interfered by cannflavins remains unknown and should be considered in future research.

403 *Therapeutic potential of cannflavins*

404 Although cannflavins are recognized to produce potent anti-inflammatory effects by inhibiting the
405 biosynthesis of various pro-inflammatory mediators, including microsomal prostaglandin E_2
406 synthase-1 (mPGES-1) and 5-lipoxygenase (5-LO) (Barrett et al., 1985; 1986; Werz et al., 2014),
407 our study cautions that these flavonoids may not be best to intervene against neuroinflammation
408 or provide pro-cognitive effects because of their impact on TrkB signaling (Jaeger et al., 2018).
409 That being said, cannflavin A and/or cannflavin B may prove to be helpful in other circumstances
410 where TrkB signaling is instead found to be overactive or dysregulated. For instance, increased
411 TrkB expression was detected in low-grade astrocytoma and glioblastoma (Wadhwa et al., 2003;
412 Assimakopoulou et al., 2007), while BDNF-induced activation of TrkB has been found to increase
413 the viability of brain-tumor stem cells isolated from glioblastoma (Lawn et al., 2015). Furthermore,
414 a study uncovered a link between the ability of glioblastoma to make less invasive cancer cells
415 around them more aggressive via the transfer of TrkB-containing exosomes, revealing this way a
416 mechanism by which these tumours can influence their environment to promote disease
417 progression and aggressiveness (Pinet al et., 2016), while other reports have shown that inhibition
418 of TrkB-associated signaling may be an effective strategy to limit the formation of astrocytomas
419 (Ni et al., 2017) as well as the survival of glioblastoma cancer cells (Pinheiro et al., 2017). Finally,
420 emerging evidence suggest that TrkB signaling could also be a therapeutic target for other cancer
421 types, including lung (Sinkevicius et al., 2014; Chen et al., 2016), breast (Choy et al., 2017;
422 Contreras-Zárate et al., 2019), and pancreatic cancer (Oyama et al., 2021). Taken together, these
423 studies suggest that targeting TrkB signaling with cannflavins may provide therapeutic benefits
424 against these cancer types. In conclusion, our study expands the range of cellular effect for

425 cannflavins beyond inflammation and supports the examination in more detail of these compounds

426 as possible anti-cancer agents.

DATA AVAILABILITY STATEMENT

The raw data supporting the conclusions of this article will be made available by the authors, without undue reservation.

ETHICS STATEMENT

The use of mice for primary neuron cultures was reviewed and approved by the University of Guelph Animal Care Committee.

CONFLICT OF INTEREST

TAA received sponsored research funding from Atlas 365 that was used for the preparation of cannflavins used in this research. The other authors declare no conflict of interest.

AUTHOR CONTRIBUTIONS

JH, AWM, BA, JYK, and JL planned and designed the experiments. CP, JYK, and TAA provided key resources, and JH, AWM, BA, and CA performed the research. JH, AWM, BA, CP, CA, and JL analyzed the data and prepared figures. JH, AWM, and JL wrote the manuscript with revisions from all other authors.

FUNDING

This work was supported by a Natural Sciences and Engineering Research Council of Canada (NSERC) Discovery Grant (401389), the Canadian Foundation for Innovation (CFI, 037755), and generous start-up funding from the University of Guelph (all to JL). A.W.M was supported by the University of Guelph (Graduate Tuition Scholarship).

ACKNOWLEDGMENTS

We wish to thank Drs. Dyanne Brewer and Armen Charchoglyan for their assistance with mass spectrometry analysis of cannflavins, as well as the NIMH Psychoactive Drug Screening Program (NIMH-PDSP) for help collecting the Tango GPCR assay results presented in this study.

REFERENCES

Assimakopoulou, M., Kondyli, M., Gatzounis, G., Maraziotis, T., Varakis, J. (2007) Neurotrophin receptors expression and JNK pathway activation in human astrocytomas. *BMC Cancer* 7,202.

Bakoyiannis, I., Daskalopoulou, A., Pergialiotis, V., Perrea, D. (2018) Phytochemicals and cognitive health: Are flavonoids doing the trick? *Biomed. Pharmacother. 190*, 1488-1497.

Barrett, M.L., Gordon, D., Evans, F.J. (1985) Isolation from Cannabis sativa L. of cannflavin–a novel inhibitor of prostaglandin production. *Biochem. Pharmacol. 34*, 2019-2024.

Barrett, M.L., Scutt, A.M., Evans, F.J. (1986) Cannflavin A and B, prenylated flavones from Cannabis sativa L. *Experientia 42*, 452-453.

Bondonno, N.P., Dalgaard, F., Kyrø, C., Murray, K., Bondonno, C.P., Lewis, J.R., Croft, K.D., Gislason, G., Scalbert, A., Cassidy, A., Tjønneland, A., Overvad, K., Hodgson, J.M. (2019) Flavonoid intake is associated with lower mortality in the Danish Diet Cancer and Health Cohort. *Nat. Commun. 10*, 3651.

Bramham, C.R., Alme, M.N., Bittins, M., Kuipers, S.D., Nair, R.R., Pai, B., Panja, D., Schubert, M., Soule, J., Tiron, A., Wibrand, K. (2010) The Arc of synaptic memory. *Exp. Brain Res. 200*, 125-140.

Brunelli, E., Pinton, G., Bellini, P., Minassi, A., Appendino, G., Moro, L. (2009) Flavonoid-induced autophagy in hormone sensitive breast cancer cells. Fitoterapia 80, 327-332.

Cazorla, M., Prémont, J., Mann, A., Girard, N., Kellendonk, C., Rognan, D. (2011) Identification of a low-molecular weight TrkB antagonist with anxiolytic and antidepressant activity in mice. *J Clin Invest. 121*, 1846-1857.

476 Chen, B., Liang, Y., He, Z., An, Y., Zhao, W., Wu, J. (2016) Autocrine activity of BDNF induced
477 by the STAT3 signaling pathway causes prolonged TrkB activation and promotes human non-
478 small-cell lung cancer proliferation. *Sci. Rep.* 6, 30404.
479 Choi, Y.H., Hazekamp, A., Peltenburg-Looman, A.M., Frédérich, M., Erkelens, C., Lefeber, A.W.,
480 Verpoorte, R. (2004) NMR assignment of the major cannabinoids and cannabiflavonoids
481 isolated from flowers of Cannabis sativa. *Phytochem. Anal. 15*, 345-354.
482 Choy, C., Ansari, K.I., Neman, J., Hsu, S., Duenas, M.J., Li, H., Vaidehi, N., Jandial, R. (2017)
483 Cooperation of neurotrophin receptor TrkB and Her2 in breast cancer cells facilitates brain
484 metastases. *Breast Cancer Res.* 19, 51.
485 Contreras-Zárate, M.J., Day, N.L., Ormond, D.R., Borges, V.F., Tobet, S., Gril, B., Steeg, P.S.,
486 Cittelly, D.M. (2019) Estradiol induces BDNF/TrkB signaling in triple-negative breast cancer
487 to promote brain metastases. *Oncogene* 38, 4685-4699.
488 Ding, S., Zhuge, W., Hu, J., Yang, J., Wang, X., Wen, F., Wang, C., Zhuge, Q. (2018) Baicalin
489 reverses the impairment of synaptogenesis induced by dopamine burden via the stimulation
490 of $GABA_AR$-TrkB interaction in minimal hepatic encephalopathy. *Psychopharmacology 235*,
491 1163-1178.
492 Eggers, C., Fujitani, M., Kato, R., Smid, S. (2019) Novel cannabis flavonoid, cannflavin A
493 displays both a hormetic and neuroprotective profile against amyloid β-mediated
494 neurotoxicity in PC12 cells: Comparison with geranylated flavonoids, mimulone and
495 diplacone. *Biochem. Pharmacol. 169*, 113609.
496 El Zein N., Badran, B.M., Sariban, E. (2007) The neuropeptide pituitary adenylate cyclase
497 activating protein stimulates human monocytes by transactivation of the Trk/NGF pathway.
498 (2007) *Cell. Signal. 19*, 152-162.

499 Flores-Sanchez, I.J., Verpoorte, R. (2008) Secondary metabolism in *Cannabis*. *Phytochem. Rev.*
500 *7*, 615-639.
501 Gundimeda, U., McNeill, T.H., Fan, T.K., Deng, R., Rayudu, D., Chen, Z., Cadenas, E.,
502 Gopalakrishna, R. (2014) Green tea catechins potentiate the neuritogenic action of brain-
503 derived neurotrophic factor: role of 67-kDa laminin receptor and hydrogen peroxide.
504 *Biochem. Biophys. Res. Commun. 445*, 218-224.
505 Gupta, V.K., You, Y., Gupta, V.B., Klistorner, A., Graham, S.L. (2013) TrkB receptor signalling:
506 implications in neurodegenerative, psychiatric and proliferative disorders. *Int J Mol Sci*. *14,*
507 10122-10142.
508 Herrera-Hernández, M.G., Ramon, E., Lupala, C.S., Tena-Campos, M., Pérez, J.J., Garriga, P.
509 (2017) Flavonoid allosteric modulation of mutated visual rhodopsin associated with retinitis
510 pigmentosa. *Sci. Rep. 7*, 11167.
511 Huang, E.J., Reichardt, L.F. (2003) Trk receptors: Roles in neuronal signal transduction. *Annu.*
512 *Rev. Biochem. 72*, 609-642.
513 Jaeger, B.N., Parylak, S.L., Gage, F.H. (2018) Mechanisms of dietary flavonoid action in neuronal
514 function and neuroinflammation. *Mol. Aspects Med. 61*, 50-62.
515 Kedrov, A.V., Durymanov, M., Anokhin, K.V. (2019) The Arc gene: Retroviral heritage in
516 cognitive functions. *Neurosci. Biobehav. Rev. 99*, 275-281.
517 Korb, E., Finkbeiner, S. (2011) Arc in synaptic plasticity: from gene to behavior. *Trends Neurosci.*
518 *34*, 591-598.
519 Kowiański, P., Lietzau, G., Czuba, E., Waśkow, M., Steliga, A., Moryś, J. (2018) BDNF: A key
520 factor with multipotent impact on brain signaling and synaptic plasticity. *Cell. Mol. Neurobiol.*
521 38, 579-593.

522 Kroeze, W.K., Sassano, M.F., Huang, X.P., Lansu, K., McCorvy, J.D., Giguère, P.M., Sciaky, N.,
523 Roth, B.L. (2015) PRESTO-Tango as an open-source resource for interrogation of the
524 druggable human GPCRome. *Nat. Struct. Mol. Biol. 22*, 362-369.
525 Lalonde, J., Reis, S.A., Sivakumaran, S., Holland, C.S., Wesseling, H., Sauld, J.F., Alural, B.,
526 Zhao, W.N., Steen, J.A., Haggarty, S.J. (2017) Chemogenomic analysis reveals key role for
527 lysine acetylation in regulating Arc stability. *Nat. Commun. 8*, 1659.
528 Lawn, S., Krishna, N., Pisklakova, A., Qu, X., Fenstermacher, D.A., Fournier, M., Vrionis, F.D.,
529 Tran, N., Chan, J.A., Kenchappa, R.S., Forsyth, P.A. (2015) Neurotrophin signaling via TrkB
530 and TrkC receptors promotes the growth of brain tumor-initiating cells. *J. Biol. Chem.*
531 290,3814-3824.
532 Lu, Y., Sun, G., Yang, F., Guan, Z., Zhang, Z., Zhao, J., Liu, Y., Chu, L., Pei, L. (2019) Baicalin
533 regulates depression behavior in mice exposed to chronic mild stress via the Rac/LIMK/cofilin
534 pathway. *Biomed. Pharmacother. 116*, 109054.
535 Meakin, S.O., MacDonald, J.I.S., Gryz, E.A., Kubum C.J., Verdim J.M. (1999) The signaling
536 adapter FRS-2 competes with Shc for binding to the nerve growth factor receptor TrkA. *J Biol*
537 *Chem. 274,* 9861-9870.
538 Moreau, M., Ibeh, U., Decosmo, K., Bih, N., Yasmin-Karim, S., Toyang, N., Lowe, H., Ngwa, W.
539 (2019) Flavonoid derivative of *Cannabis* demonstrates therapeutic potential in preclinical
540 models of metastatic pancreatic cancer. *Front. Oncol. 9*, 660.
541 Ni, J., Xie, S., Ramkissoon, S.H., Luu, V., Sun, Y., Bandopadhayay, P., Beroukhim, R., Robers,
542 T.M. Stiles, C.D., Segal, R.A., Ligon, K.L., Hahn, W.C., Zhao, J.J. (2017) Tyrosine receptor
543 kinase B is a drug target in astrocytomas. *Neuro Oncol.* 19, 22-30.
544

545 Oyama, Y., Nagao, S., Na, L., Yanai, K., Umebayashi, M., Nakamura, K., Nagai, S., Fujimura,
546 A., Yamasaki, A., Nakayama, K., Morisaki, T., Onishi, H. (2021) TrkB/BDNF signaling could
547 be a new therapeutic target for pancreatic cancer. Anticancer Res. 41, 4047-4052.
548 Ortega, J.T., Parmar, T., Jastrzebska, B. (2019) Flavonoids enhance rod opsin stability, folding,
549 and self-association by directly binding to ligand-free opsin and modulating its conformation.
550 *J. Biol. Chem.* 294, 8101-8122.
551 Pan, M., Han, H., Zhong, C., Geng, Q. (2012) Effects of genistein and daidzein on hippocampus
552 neuronal cell proliferation and BDNF expression in H19-7 neural cell line. *J. Nutr. Health*
553 *Aging 16*, 389-394.
554 Panche, A.N., Diwan, A.D., Chandra, S.R. (2016) Flavonoids: an overview. *J. Nutr. Sci. 5*, e47.
555 Pinet, S., Bessette, B., Vedrenne, N., Lacroix, A., Richard, L., Jauberteau, M.O., Battu, S., Lalloué,
556 F. (2016) TrkB-containing exosomes promote the transfer of glioblastoma aggressiveness to
557 YKL-40-inactivated glioblastoma cells. *Oncotarget* 7,50349-50364
558 Pinheiro, K.V., Alves, C., Buendia, M., Gil, M.S., Thomaz, A., Schwartsmann, G., de Farias, C.B.,
559 Roesler, R., Bowman, R.L., Wang, Q., Carro, A., Verhaak, R.G., Squatrito, M. (2017)
560 Targeting tyrosine receptor kinase B in gliomas. *Neuro Oncol.* 19,138-139.
561 Qian, X., Riccio, A., Zhang, Y., Ginty, D.D. (1998) Identification and characterization of novel
562 substrates of Trk receptors in developing neurons. *Neuron. 21*, 1017–1029.
563 Rajagopal, R., Chao, M.V. (2006) A role for Fyn in Trk receptor transactivation by G-protein-
564 coupled receptor signaling. *Mol. Cell Neurosci. 33*, 36-46.
565 Rajagopal, R., Chen, Z.Y., Lee, F.S., Chao, M.V. (2004) Transactivaion of Trk neurotrophin
566 receptors by G-protein-coupled receptor ligands occurs on intracellular membranes. *J.*
567 *Neurosci. 24*, 6650-6658.

568 Rea, K.A., Cararetto, J.A., Al-Abdul-Wahid, M.S., Sukumaran A., Geddes-McAlister J., Rothstein
569 S.J., Akhtar T.A. (2019) Biosynthesis of cannflavins A and B from Cannabis sativa L.
570 *Phytochemistry*, *164*, 162-171.
571 Sinkevicius, K.W., Kriegel, C., Bellaria, K.J., Lee, J., Lau, A.N., Leeman, K.T., Zhou, P., Beede,
572 A.M., Fillmore, C.M., Caswell, D., Barrios, J., Wong, K.K., Sholl, L.M., Schlaeger, T.M.,
573 Bronson, R.T., Chirieac, L.R., Winslow, M.M.m Gaihis, M.C., Kim, C.F. (2014)
574 Neurotrophin receptor TrkB promotes lung adenocarcinoma metastasis. *Proc. Natl. Acad. Sci.*
575 *U.S.A.* 111, 10299-10304.
576 Vauzour, D., Vafeiadou, K., Rodriguez-Mateos, A., Rendeiro, C., Spencer, J.P. (2008) The
577 neuroprotective potential of flavonoids: a multiplicity of effects. *Genes Nutri. 3*, 115-226.
578 Wadhwa, S., Nag. T.C., Jindal, A., Kushwaha, R., Mahapatra, A.K., Sarkar, C. (2003) Expression
579 of the neurotrophin receptors Trk A and Trk B in adult human astrocytoma and glioblastoma.
580 *J. Biosci.* 28, 181-188.
581 Werz, O., Seegers, J., Schaible, A. M., Weinigel, C., Barz, D., Koeberle, A., Allegrone, G.,
582 Pollastro, F., Zampieri, L., Grassi, G., Appendino, G. (2014). Cannflavins from hemp sprouts,
583 a novel cannabinoid-free hemp food product, target microsomal prostaglandin E_2 synthase-1
584 and 5-lipoxygenase. Pharmanutr. 2, 53-60.

A

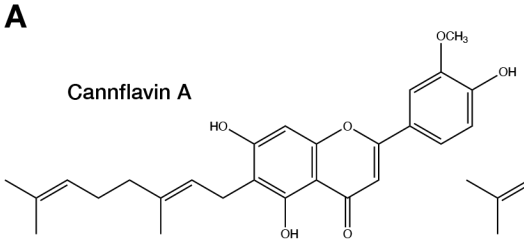

B

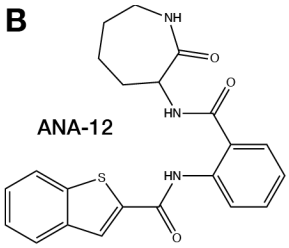

C

Name	Flavanoid class	Structure	Reported impact on BDNF-induced Arc expression in mouse primary cortical neurons at a concentration of 16.7μM (Lalonde et al., 2017)
(–)-Epigallocatechin gallate (EGCG)	Flavanol	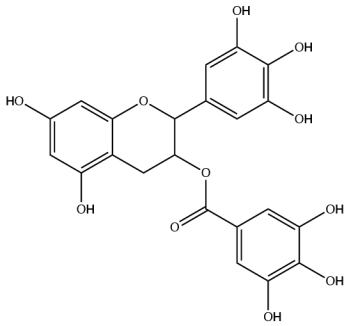	**1.9** fold-change (normalized value to BDNF baseline + vehicle treated cells)
Baicalin	Flavone	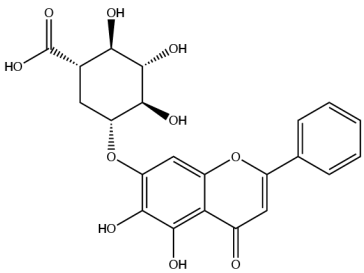	**1.8** fold-change
Daidzein	Isoflavone	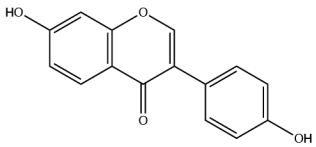	**2.1** fold-change
Genistein	Isoflavone	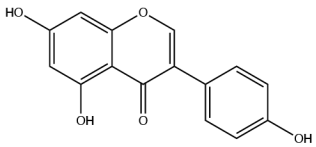	**1.6** fold-change
7,8-Dihydroxyflavone (7,8-DHF)	Flavone	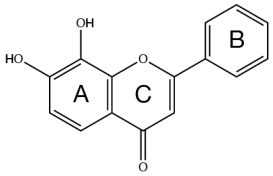	**1.7** fold-change

585

586 **Figure 1. Chemical structures of key compounds. A)** Chemical structure for cannflavin A and
587 cannflavin B. **B)** Structure for the small molecule TrkB inhibitor ANA-12. **C)** Table presenting
588 flavonoids organized by name, flavonoid class, chemical structure, and impact of BDNF-induced
589 Arc expression in mouse primary cortical neurons as reported in Lalonde et al. (2017). Position of
590 each ring is labeled for 7,8-dihydroxyflavone.
591
592

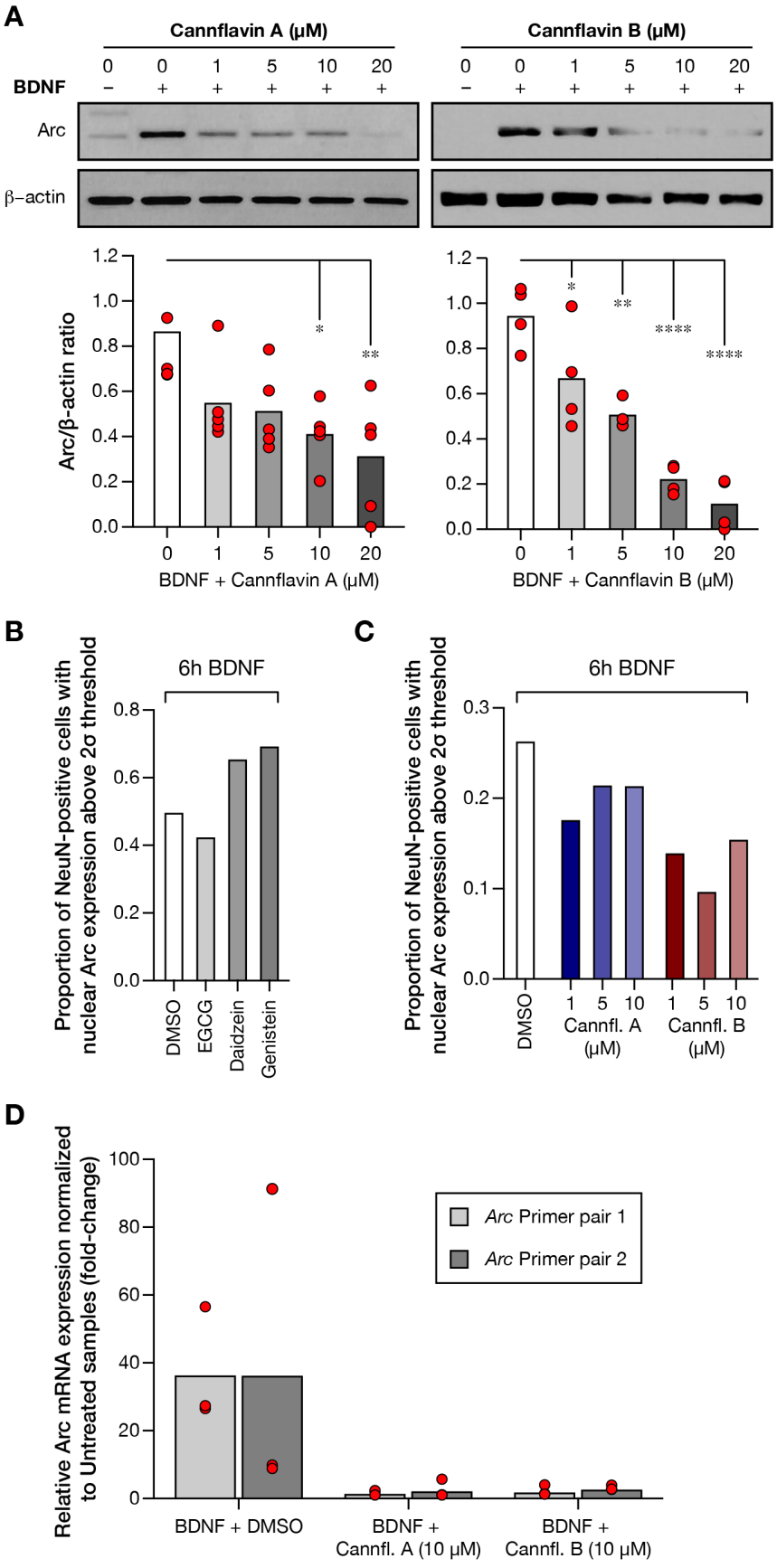

593

Figure 2. Cannflavin A and cannflavin B decrease BDNF-induced Arc protein and mRNA levels in mouse primary cortical neurons. A) Western blot and corresponding densitometry analysis showing Arc protein abundance in mouse primary cortical cultures when treated with BDNF and various concentrations (0, 1, 5, 10, 20 μM) of cannflavin A (left) or cannflavin B (right). β-actin was used a loading control and graphs show mean of Arc/β-actin ratio for each condition. Biological replicates: n = 5 (cannflavin A), n = 4 (cannflavin B). One way ANOVA revealed a significant decrease in the abundance of Arc with increasing cannflavin concentrations. Cannflavin A ($F_{4,20} = 4.568$, $p = 0.0088$), Tukeys post-hoc test, * $p < 0.05$, ** $p < 0.001$. Cannflavin B ($F_{4,15} = 24.07$, $p < 0.0001$), Tukeys post-hoc test, * $p < 0.05$, ** $p < 0.001$, **** $p < 0.0001$. **B)** Quantification of immunocytochemistry coverslips treated with various flavonoids (EGCG, daidzein, and genistein; all 10 μM final concentration). Quantification was completed by using a ratio of MAP2-positive cells with nuclear Arc above the 2σ nuclear Arc pixel intensity in the control condition (BDNF treatment alone). **C)** Quantification of immunocytochemistry coverslips treated with various concentrations (0, 1, 5, 10 μM) of cannflavin A (blue bars) or cannflavin B (red bars). Quantification was completed similar to B. **D)** Quantitative real-time PCR *Arc* mRNA analysis using two Arc primer pairs shows a decrease in *Arc* transcripts when treated with 10 μM of cannflavin A or cannflavin B, relative to cells treated with BDNF alone.

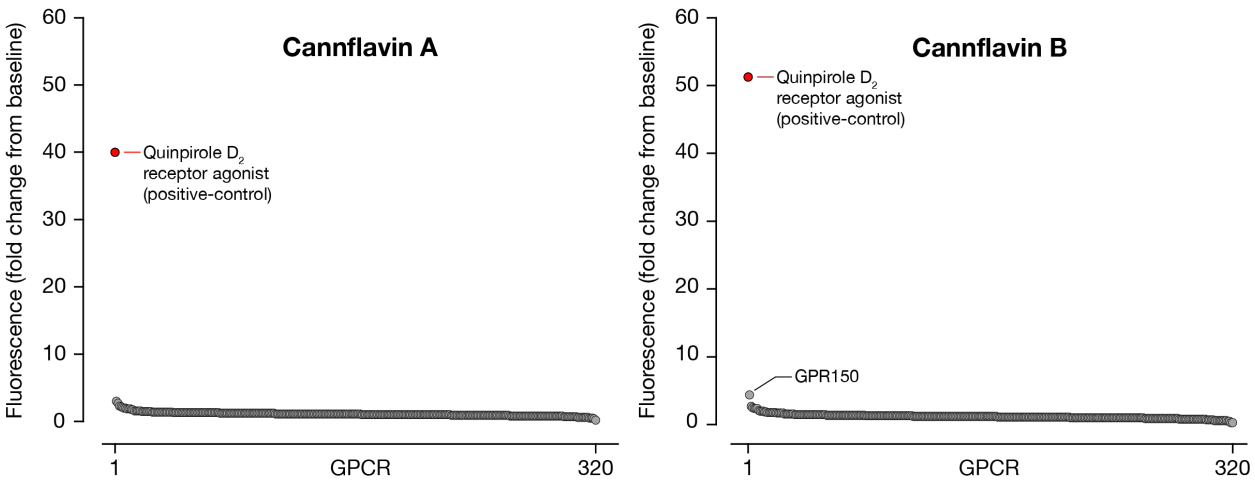

611
612

613 **Figure 3. Cannflavins do not stimulate G protein-coupled receptors signaling.** Data for 320
614 GPCRs are presented as an average fold change from baseline upon compound addition.
615 Application of quinpirole to D2 receptor is used as positive control in each plate. Compounds were
616 used at 10 μM and all tests run in quadruplicate.

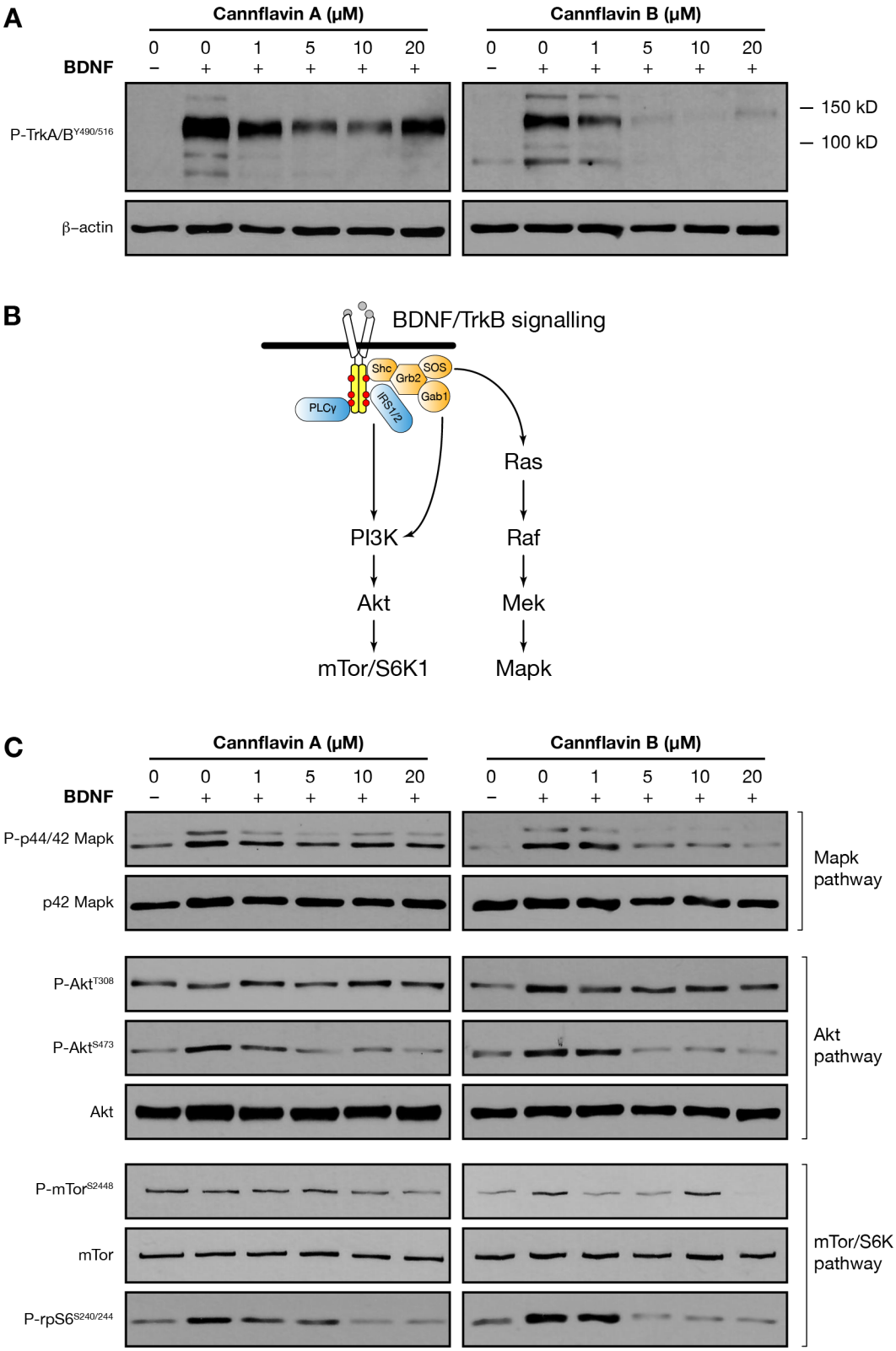

620 **Figure 4. Cannflavin A and cannflavin B decrease activation of downstream pathways of**
621 **TrkB. A)** Western blot analysis showing phosphorylation of TrkB when treated with BDNF and
622 various concentrations (0, 1, 5, 10, 20 μM) of cannflavin A (left) or cannflavin B (right). β-actin
623 was used a loading control. **B)** Simplified schematic of BDNF activation of TrkB receptors and
624 downstream signaling pathways. **C)** Western blot analysis showing phosphorylation of Mapk, Akt,
625 and mTor proteins when treated with various concentrations (0, 1, 5, 10, 20 μM) of cannflavin A
626 (left) or cannflavin B (right).

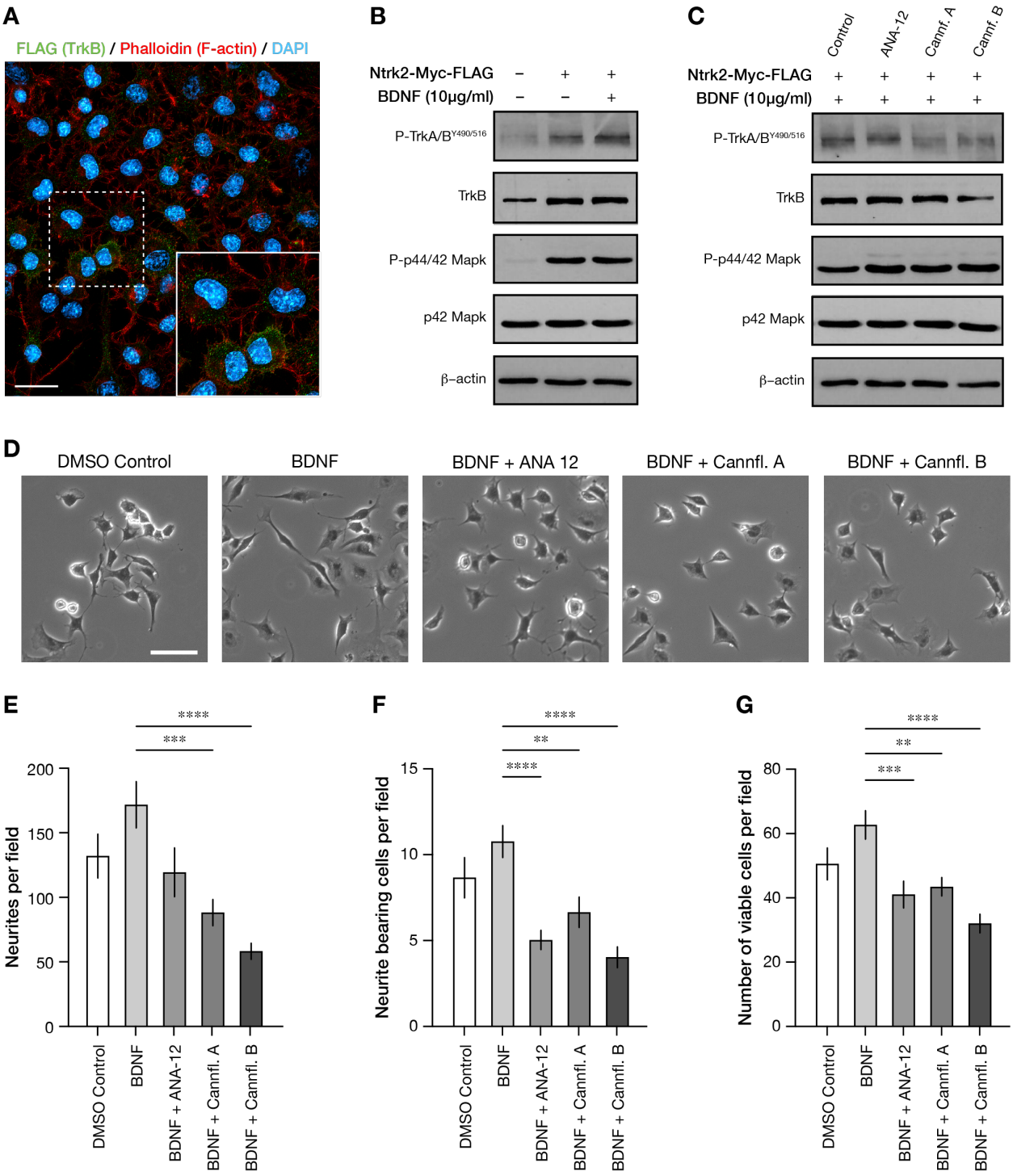

Figure 5. Cannflavin A and cannflavins B reduces BDNF-induced neurite outgrowths in neuroblastoma cells. A) Neuro2a cells were transfected to stably express Ntrk2-Myc-FLAG. Immunocytochemistry was completed to validate that the cells were successfully transfected. Scale

bar = 20 μM. **B)** Western blot analysis showing phosphorylation of TrkB and Mapk in regular Neuro2a cells compared to those stably expressing Ntrk2-Myc-FLAG. β-actin was used a loading control. **C)** Western blot analysis showing phosphorylation of TrkB and Mapk when treated with 10 μM of ANA-12, cannflavin A, or cannflavin B with the addition of BDNF (10 μg/mL). The small-molecule non-competitive TrkB antagonist ANA-12 was used as a positive control (Cazorla et al., 2011) and β-actin was used as a loading control. **D)** Phase contrast images of Ntrk2-Myc-FLAG Neuro2as treated with or without BDNF (10 μg/mL) and 10 μM of ANA-12, cannflavin A, or cannflavin B. Scale bar = 50 μm. Images were quantified by counting **E)** total number of neurites, and **F)** total number of cells bearing neurites twice the length of cell body, and **G)** number of viable cells per imaged area. One-way ANOVA was used to analyze data. Total number of neurites ($F_{4,150} = 8.264, p < 0.001$); total number of cells bearing neurites ($F_{4,150} = 9.433, p < 0.001$); number of viable cells ($F_{4,150} = 8.071, p < 0.001$). Dunnett's multiple comparisons test to BDNF condition, * $p < 0.05$; ** $p < 0.01$; *** $p < 0.001$; *** $p < 0.0001$. Graphs represent mean ±SEM.

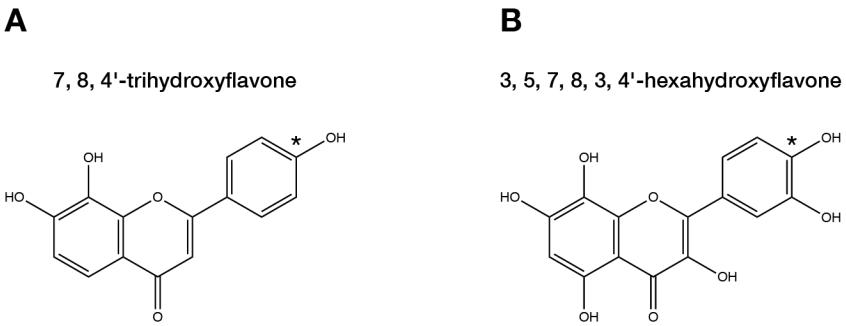

Figure 6. Chemical structure of 7,8-dihydroxyflavone derivatives reported to block TrkB signaling in Liu and colleagues (2010). Asterisk indicates hydroxylated 4' position on B ring of each compound.

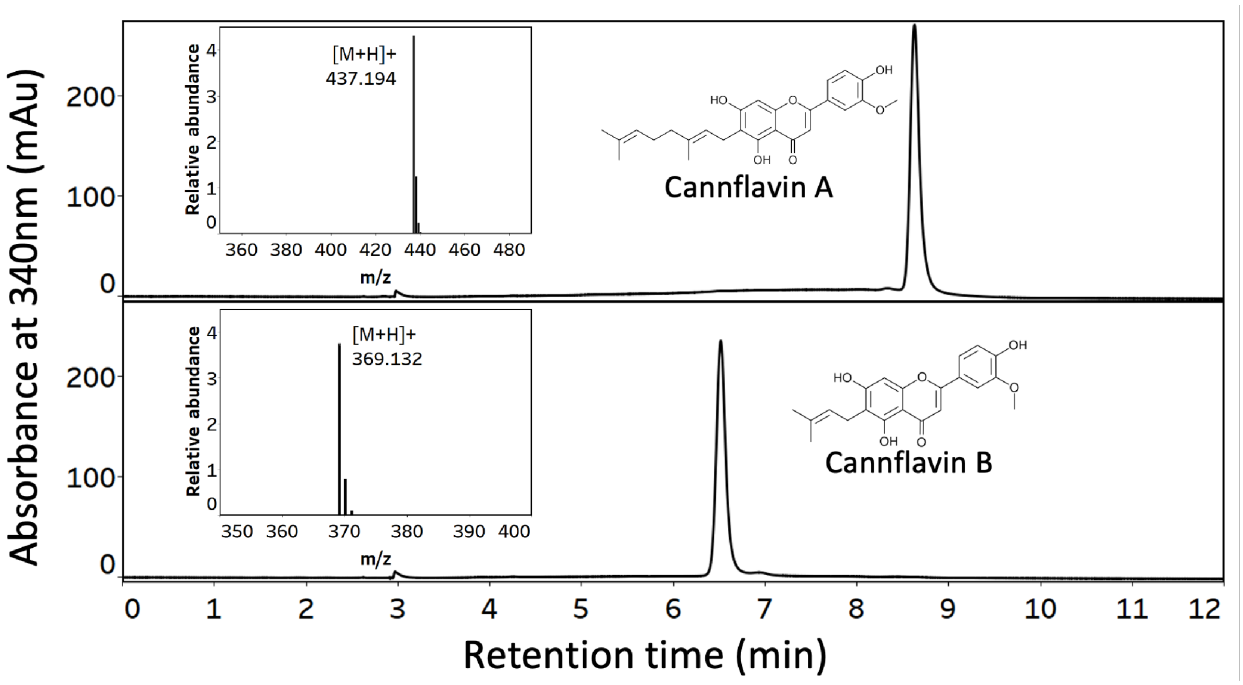

650
651

652 **Supplementary Figure 1. Enzymatic production of cannflavin A and cannflavin B.**
653 Representative chromatograms illustrating pooled fractions of cannflavin A (top) and cannflavin
654 B (bottom) quantified by DAD at 340 nm. Both Q-TOF mass spectra (inset) are consistent with
655 the expected m/z of 6-geranyl chrysoeriol and 6-dimethylallyl chrysoeriol or cannflavins A and B,
656 respectively.

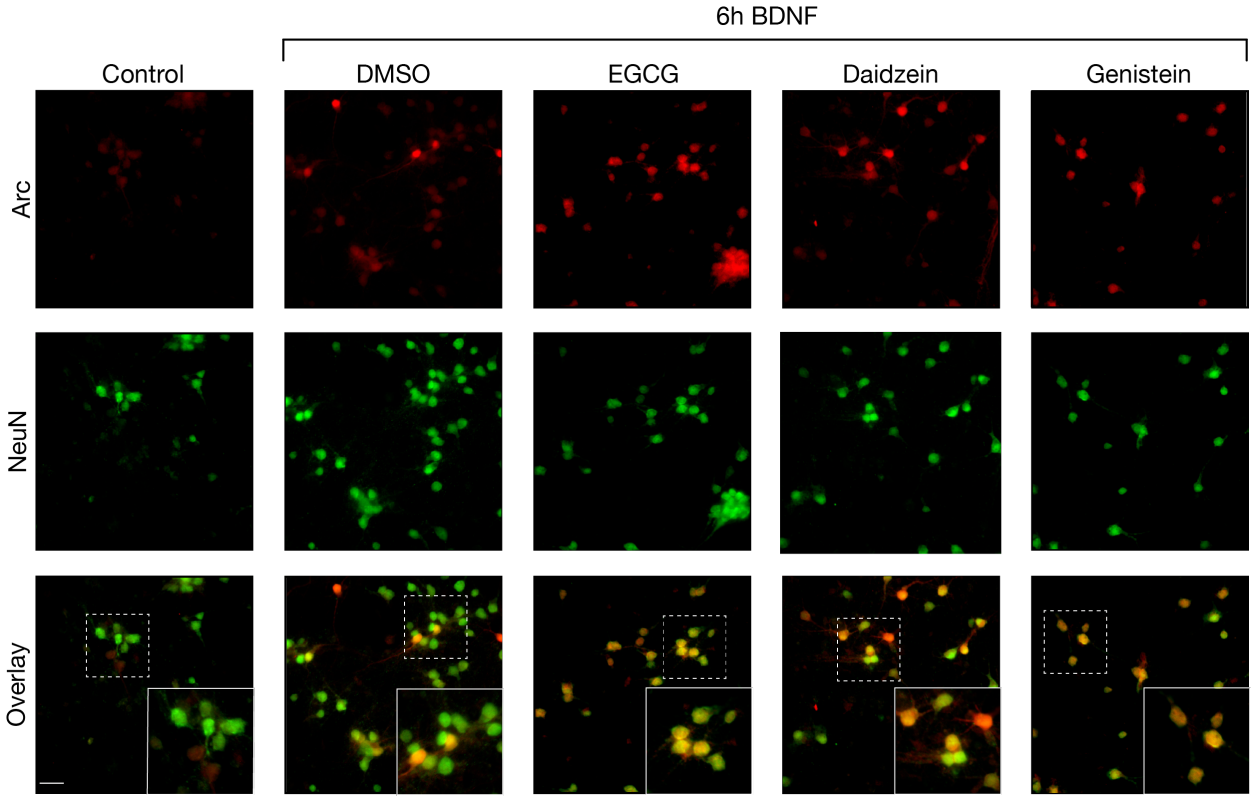

Supplementary Figure 2. Effect of other flavonoids on BDNF-induced Arc expression level in mouse primary cortical neurons. DIV14 cortical neurons were treated with BDNF for 6 h along with ECGC, daidzein, or genistein (final concentration 10 μM). DMSO was used as control. Representative immunostaining of Arc (red fluorophore) in untreated primary cortical neurons and cells that were treated with BDNF and other compounds for 6 h. Consistent with data reported in Lalonde and colleagues (2017), daidzein and genistein increased Arc abundance at the tested concentration. Cells were co-immunostained with the neuronal marker NeuN (green fluorophore) to confirm specificity of staining to neurons. The high-magnification bottom-right insets in each panel show that Arc immunostaining in a BDNF-treated culture is particularly abundant in the nuclear compartment at the 6 h time point. Scale bar = 50 μM.

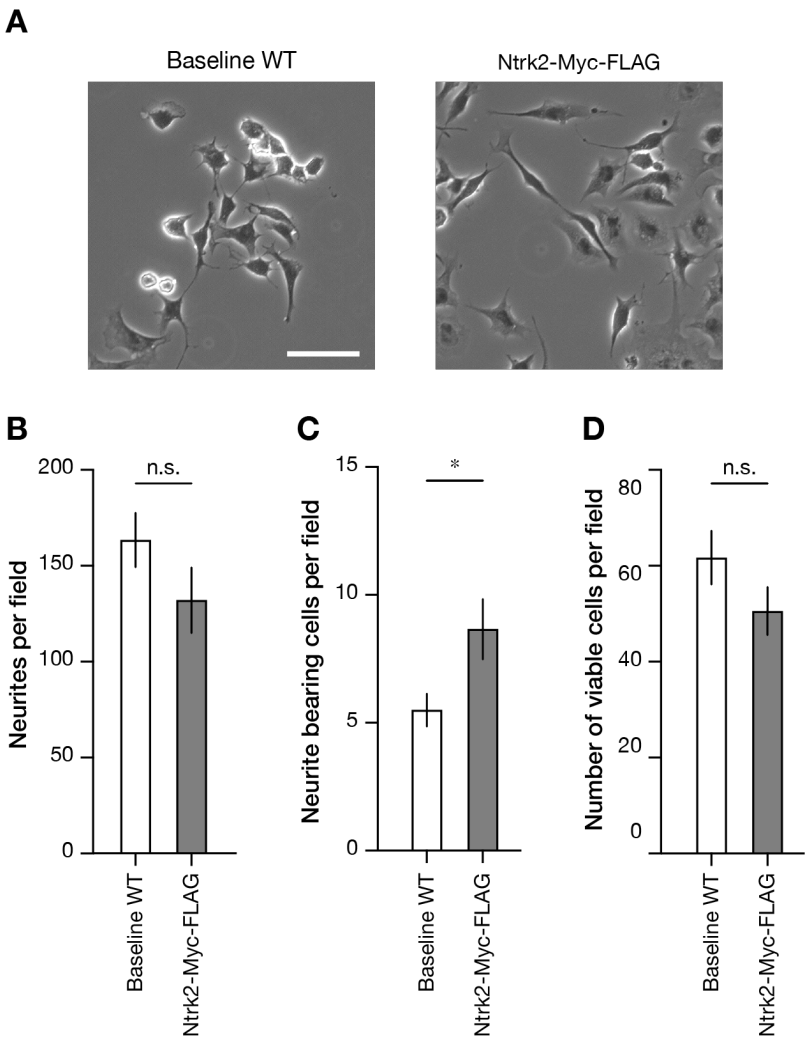

Supplementary Figure 3. Stable overexpression of Myc-FLAG tagged TrkB increases neurite outgrowths and survival in Neuro2a cells. A) Phase contrast images of wild-type (WT, left) and stably overexpressing Ntrk2-Myc-FLAG (right) Neuro2a cells. Images were quantified by counting **B)** total number of neurites, **C)** total number of cells bearing neurites twice the length of cell body, and **D)** number of viable cells per imaged area. * $p < 0.05$, two-tailed unpaired *t*-test. Graphs represent mean ±SEM.

677 **Supplementary Table. GPCRome cannflavins report.** List of all 320 GPCRs tested in the

678 PRESTO-Tango assay.